Received: 17 December 2019 | Revised: 19 March 2020 | Accepted: 12 April 2020
DOI: 10.1002/aoc.5771

FULL PAPER

Applied Organometallic Chemistry WILEY

Pd(0) complex of fuberidazole modified magnetic nanoparticles: A novel magnetically retrievable high-performance catalyst for Suzuki and Stille C-C coupling reactions

Kheirollah Nouri | **Mitra Ghassemzadeh** | **Farshid Mohsenzadeh** | **Maryam Afsharpour**

Department of Inorganic Chemistry, Chemistry & Chemical Engineering Research Center of Iran, Pajoohesh Blvd., 17th Km of Tehran–Karaj Highway, Tehran, 14968-13151, Iran

Correspondence
Mitra Ghassemzadeh, Department of Inorganic Chemistry, Chemistry & Chemical Engineering Research Center of Iran, Pajoohesh Blvd., 17th Km of Tehran–Karaj Highway, Tehran 14968-13151, Iran.
Email: mghassemzadeh@ccerci.ac.ir

Fuberidazole has been successfully immobilized onto nano-Fe_3O_4 supported (3-chloropropyl)trimethoxysilane (3-CPTS) leading to a novel functionalized magnetic nanoparticle (FB/MNP). The Pd(0) complex, Pd-FB/MNP, was prepared by grafting Pd $(OAc)_2$ on FB/MNP and subsequent reduction of a synthesized Pd (II) complex using $NaBH_4$. Pd-FB/MNP has been characterized by FT-IR, SEM, TGA, XRD, ICP, EDS, BET and VSM. The Pd(0) complex proved to be an efficient phosphine- and halide-free recyclable heterogeneous catalyst for Suzuki as well as for Stille C-C coupling reactions showing high catalytic activity (up to 98%). Its catalytic activity in both reactions has been studied in PEG-400 as a green solvent. Besides, the selectivity of aryl iodide and aryl bromide over aryl chloride is observed during the C-C coupling reaction. The catalyst could be recovered easily from the reaction mixture using an external magnet device and recycled several times without considerable loss in activity. Additionally, the results of a palladium leaching test of the nano-catalyst demonstrate that no leaching of Pd took place during the C-C coupling process making the procedure environmentally friendly.

KEYWORDS
carbon–carbon coupling reactions, magnetic nanoparticle, Pd(0) complex of fuberidazole, Stille reaction, Suzuki reaction

1 | INTRODUCTION

In the past few decades, the design, synthesis, and development of heterogeneous reusable catalysts have attracted considerable attention in organic chemistry.[1–3] In order to reach this important goal, the homogeneous active sites of catalysts has already been immobilized on various supports.[4–8] Recently, magnetic nanoparticles have been employed as convenient supports for the preparation of heterogeneous catalysts.[9] In general, nanoparticles possess several attractive features such as high stability, high specific surface area, non-toxicity, ease of surface modification and tunable particle sizes.[10,11] The main advantage of magnetic nanoparticles over other high surface area supports, remains in their facile recovery and recyclability from the reaction mixture; since no conventional filtration or purification is required.[12–14] In other words, the use of

https://doi.org/10.1002/aoc.5771

a simple external magnetic field along with minimal workup procedures leads to a greener protocol from an academic and industrial vantage point.[15]

Carbon–carbon coupling reactions have attracted a great deal of attention in the preparation of natural products, agrochemicals and pharmaceuticals[16] such as Atazanavir,[17] Vancomycin[18] and MK2 inhibitors.[19] Suzuki and Stille Pd-catalyzed cross-coupling reactions represent two powerful and most widely used methods in organic chemistry for the formation of C-C bonds. In the classical method, these reactions have been catalyzed by Pd-based Lewis acids and complexes containing phosphine- and chlorine-based ligands having air and/or moisture-sensitive properties with high toxicity. Besides, the main problem encountered with these homogeneous catalysts remains in Pd catalyst recovery and metal ion leaching triggering undesired metal contamination of the products.[20] To minimize and overcome these issues, the design of Pd-based catalysts *via* heterogenization has become a necessity.[21,22] In this regard, various palladium-immobilized materials have been designed to achieve waste-free processes.[23]

Benzimidazoles are therapeutically active building blocks, which have been extensively investigated in the field of the pharmaceutical industry and drug design.[24] Their coordination behavior towards transition metal ions have different pharmacological and biological applications.[25] Moreover, their derivatives incorporating a fluorescent aromatic moiety, usually act as chelating sites toward metal ions and are generally utilized as chemical tools for the recognition of metal ions.[26,27] So far, a range of 2-aryl substituted benzimidazole-based moieties (in order to chelate to transition metal ions) have been used as a receptor for fluorescent sensing, e.g. 2-(2′-hydroxyphenyl)-benzimidazole,[28–31] 2-(2′-aminophenyl)-benzimidazole,[32–35] 2-(5-R-1H-benzimidazol-2-yl)-benzene-1,4-diols.[36,37]

Fuberidazole (2-(2′-furyl)-1H-benzimidazole) is a well-known antifungal agrochemical. It is essentially used for the treatment of seeds particularly against *Fusarium* spp as an agricultural plant pathogen.[38–40] The structure of fuberidazole contains two aromatic heterocycles: a 2-substituted benzimidazole moiety and a 2-furyl one. While this biheterocyclic compound has the potential to coordinate to metal ions, a survey in the literature revealed that there is no report on Pd complexes containing fuberidazole as a chelating agent.

Taking into account the importance of magnetic nanoparticles as a sustainable support for chemical transformations[41–43] and our interest in the design of novel Pd-complexes[44–47] together with the use of fuberidazole as a new benzimidazole-based ligand, herein, we wish to report the preparation and characterization of a novel Pd(0) complex supported on functionalized Fe_3O_4 nanoparticles. In addition, the viability of this material as a recyclable heterogeneous catalyst is studied for the synthesis of biphenyl derivatives under Suzuki and Stille C-C coupling reaction conditions.

2 | EXPERIMENTAL SECTION

2.1 | Materials and methods

All chemicals were purchased from Merck, Aldrich or Fluka and used without further purification. Fe_3O_4 nanoparticles, (3-chloropropyl)trimethoxysilane (3-CPTS) modified Fe_3O_4 nanoparticles (3-CPTS/Fe_3O_4) and fuberidazole (FB) have been prepared according to literature.[48–50]

Powder X-ray Diffraction (XRD) of the catalyst was performed on a PW 1730 instrument from PHILIPS Company with Cu K_α-radiation from $2\theta = 5$ to $80\ ^\circ$ at 40 kV and 30 mA (scan step: 0.04 °/sec). Fourier transform infrared (FT-IR) spectra were recorded on a VRTEX 70 model Bruker FT-IR spectrometer using KBr Pellets (4000–400 cm^{-1}). Energy-dispersive X-ray spectroscopy (EDS) and scanning electron microscopy (SEM) were carried out on a FEI Quanta 200 scanning electron microscopy (using an accelerating voltage of 25 kV). Thermogravimetric analyses (TGA) of the compounds were carried out on a Perkin Elmer Pyris Diamond Thermogravimetric Analyzer (temperature range: 30–800 °C, heating rate: 10 °C/min). Melting points were determined using the Griffin melting point apparatus and are uncorrected. The vibrating sample magnetometer (VSM) measurements were performed using a MDKFD vibrating-sample magnetometer (by an external field of up to 8 kOe). The Pd content of the compound was determined by inductively coupled plasma optical emission spectrometry (ICP-OES; PerkinElmer optima 8000).

2.2 | Preparation of the catalyst

2.2.1 | Preparation of FB/MNP

Fuberidazole (FB, 2 mmol) was added to a suspension of 3-CPTS/Fe_3O_4 (1 g) in toluene (50 ml) and stirred for 32 hr at 80 °C under N_2 atmosphere. The resulting residue was separated by magnetic decantation, washed with ethanol (3 × 10 ml) and air dried at room temperature to give functionalized FB/MNP.

2.2.2 | One-pot preparation of Pd-FB/MNP

Palladium acetate (0.25 g, 1.1 mmol) was added to a suspension of FB/MNP (0.5 g) in ethanol (25 ml) and stirred for 20 hr under reflux conditions. $NaBH_4$ (0.19 g, 0.5 mmol) was added to the reaction mixture and refluxed for further 2 hr. The resulting residue was separated by a magnetic decantation method using an external magnetic bar, washed with ethanol (3 × 10 ml) and allowed to dry at room temperature.

2.3 | General procedure for the catalytic reactions

2.3.1 | Experimental procedure for the Suzuki reaction

In a round bottom flask (25 ml), a mixture of phenylboronic acid (1 mmol), aryl halide (1 mmol), sodium carbonate (3 mmol), Pd-FB/MNP (15 mg), and PEG-400 (1 ml) was stirred at 80 °C for an appropriate reaction time. After completion of the reaction (monitored by TLC using *n*-hexane/acetone (8:2) as eluent), the reaction mixture was diluted with water (15 ml) and diethyl ether (2 ml). The heterogeneous catalyst was removed from the reaction mixture using an external magnetic bar and was air-dried before being used in the next cycle. The reaction mixture was extracted with diethyl ether (15 ml). The organic layer was washed with water and dried over anhydrous sodium sulfate. The solvent was then evaporated to afford pure products.

2.3.2 | Experimental procedure for the Stille reaction

The same procedure as in the Suzuki reaction was carried out using triphenyltin chloride (0.5 mmol) instead of phenylboronic acid.

3 | RESULTS AND DISCUSSION

3-CPTS/Fe_3O_4 was prepared from the reaction of Fe_3O_4 nanoparticles with 3-CPTS and was used as a support for the preparation of fuberidazole functionalized magnetic nanoparticles (FB/MNP). Eventually, the reaction of palladium (II) acetate with FB/MNP followed by the reduction lof Pd (II) moieties using $NaBH_4$ in EtOH by a one-pot two-step reaction gave Pd-FB/MNP (Scheme 1).

The synthesized Pd-FB/MNP is an air-stable solid. It was characterized by powder X-ray diffraction (XRD),

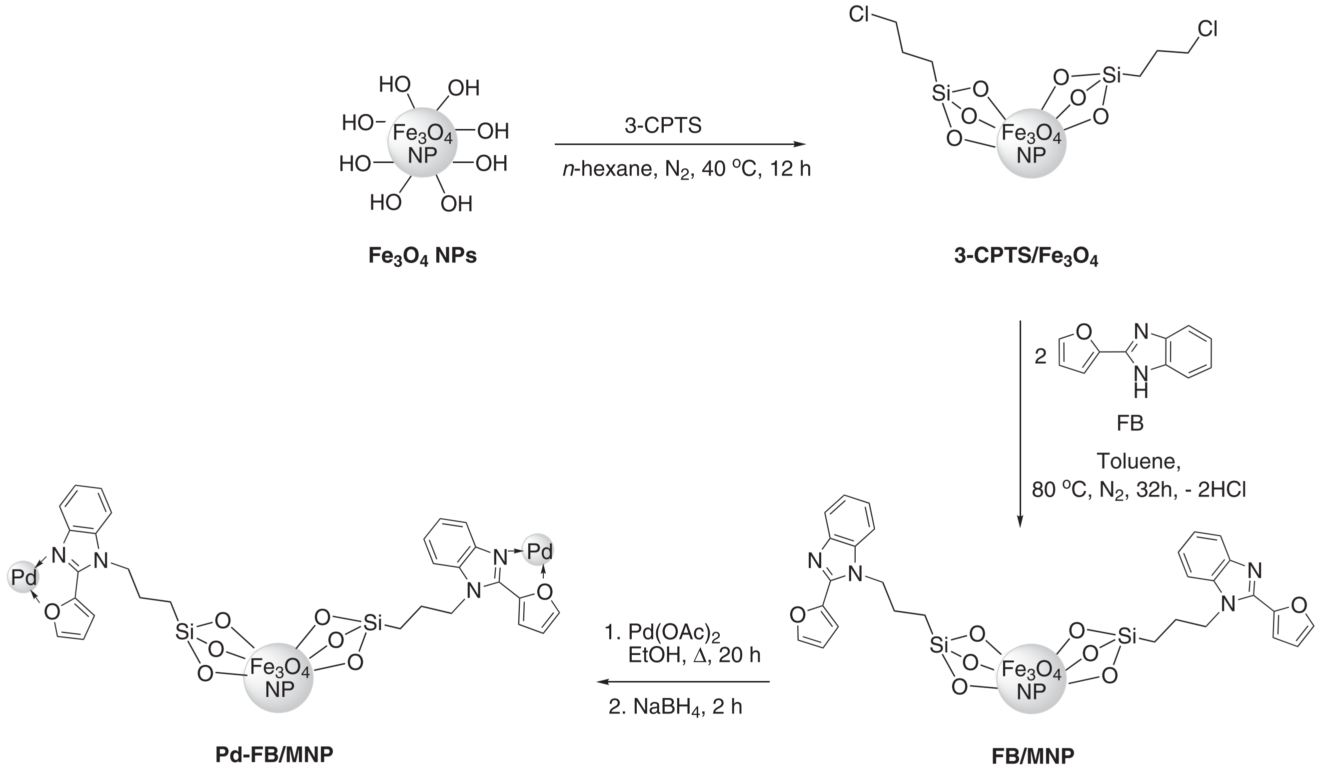

SCHEME 1 Route to the preparation of Pd-FB/MNP

scanning electron microscopy (SEM), energy-dispersive X-ray spectroscopy (EDS), inductively coupled plasma (ICP), thermogravimetric analysis (TGA), Fourier transform infrared spectroscopy (FT-IR), nitrogen adsorption–desorption isotherms and vibrating sample magnetometer (VSM).

3.1 | Characterization of Pd-FB/MNP

The XRD patterns of Fe_3O_4 nanoparticles, 3-CPTS/Fe_3O_4, FB/MNP and Pd-FB/MNP are shown in Figure 1. The XRD pattern of Fe_3O_4 showed peaks at 2θ values of 30.9 °, 35.5 °, 44.2 °, 53.7 °, 57.8 ° and 62.4 ° related to the crystal planes in Fe_3O_4 cubic lattice, which were in agreement with Fe_3O_4 standard data (JCPDS-No. 85–1436). The same template has also been observed in the XRD pattern of 3-CPTS/Fe_3O_4, FB/MNP and Pd-FB/MNP confirming the intactness of Fe_3O_4 nanostructure after modification. The XRD pattern of Pd-FB/MNP showed the reflections at 2θ = 39.2 °, 46.3 ° and 67.5 °, ascribed to the reflections of the (111), (200) and (220) diffraction planes for the Pd(0) phase (JCPDS-No. 46–1043). These three new absorptions confirm that palladium exists solely in the form of Pd(0), not Pd (II).

The SEM images revealed that Pd-FB/MNP has a quasi-spherical morphology with a very homogeneous particle size distribution. This novel material has an average diameter of 17 nm (Figure 2).

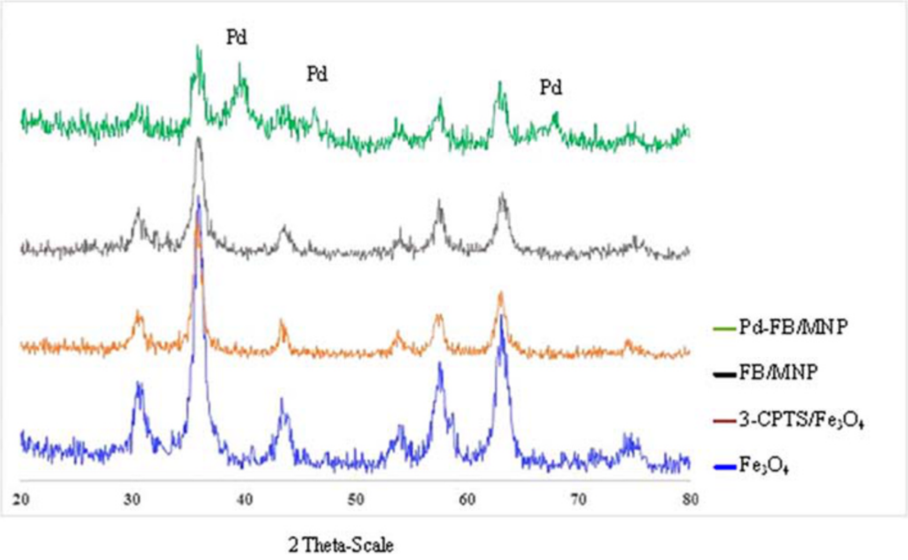

FIGURE 1 The powder XRD patterns of Fe_3O_4 nanoparticles, 3-CPTS/Fe_3O_4, FB/MNP and Pd-FB/MNP

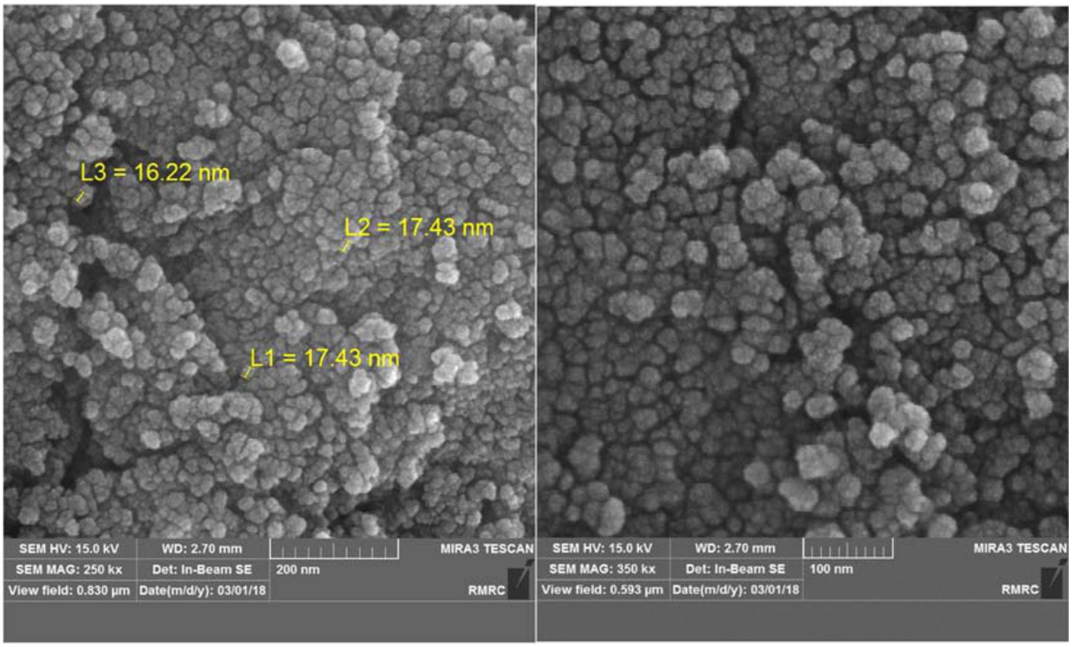

FIGURE 2 SEM images of Pd-FB/MNP

The EDS analysis carried out on Pd-FB/MNP confirmed also the presence of Fe, O, Si, C, N, and Pd with the weight percentage of 38.53, 25.89, 0.57, 10.68, 2.25, and 22.08, respectively (Figure 3). These results indicate that Pd has been anchored to FB/MNP. The exact amount of palladium in Pd-FB/MNP was found to be 1.84×10^{-3} mol g^{-1} based on the results obtained from inductively coupled plasma optical emission spectrometry (ICP-OES).

Functionalization of the Fe_3O_4 nanoparticles with organic layers was also verified by the FT-IR technique. According to the FT-IR spectra of Fe_3O_4 nanoparticles, 3-CPTS/Fe_3O_4, FB/MNP and Pd-FB/MNP (Figure 4), the stretching vibrations of Fe-O moieties were observed by a strong absorption at *ca* 580 cm^{-1}.

Symmetrical- and asymmetrical modes of the surface OH groups were observed at 3420–3550 cm^{-1} in FT-IR spectrum of all compounds (Figure 4a). Modification of Fe_3O_4 nanoparticles with 3-CPTS was confirmed by absorption at 2947 cm^{-1} and 1087 cm^{-1}, which are related to C-H– and Si-O stretching vibration, respectively. The vibration bands in FT-IR spectrum of FB/MNP observed at 1404–1440 cm^{-1} and 1628 cm^{-1} could be assigned to C-N–, C=C– and C=N stretching vibrations, respectively, confirming the successful synthesis of FB/MNP.[49]

Thermogravimetric analysis (TGA) has been used to determine the thermal degradation behavior of synthesized compounds. The thermal analysis has been performed on all samples by heating the compounds in the temperature range of 25–800 °C in air. The TGA curves of the compounds show the mass loss of the supported functional groups upon increasing the temperature. The TGA curve of all compounds (Figure 5) shows a small weight loss (*ca.* 5%) at temperatures below 200 °C, which can be assigned to the dehydration of the surface OH groups and removal of the physically adsorbed solvent in these compounds. In the TGA curve of Fe_3O_4, the small weight loss in higher temperature (>300 °C) corresponds to the thermal crystal phase transformation of Fe_3O_4. The weight loss in the range of 200–800 °C observed in the TGA curves of 3-CPTS/Fe_3O_4, FB/MNP and Pd-FB/MNP is 13%, 17% and 19%, respectively and might be related to the decomposition and removal of organic functional groups on Fe_3O_4 surface.

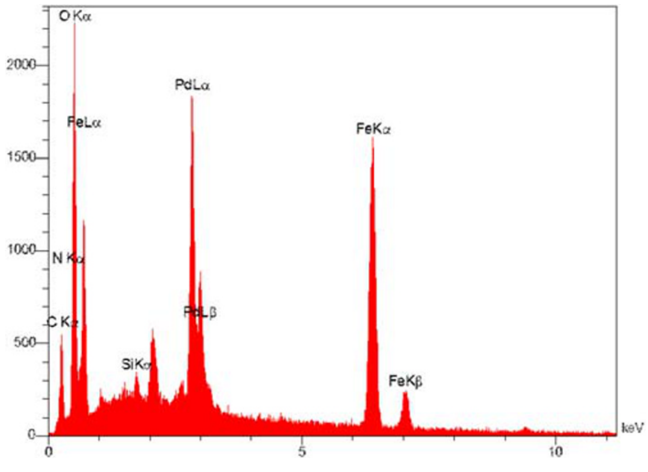

FIGURE 3 EDS analysis of Pd-FB/MNP

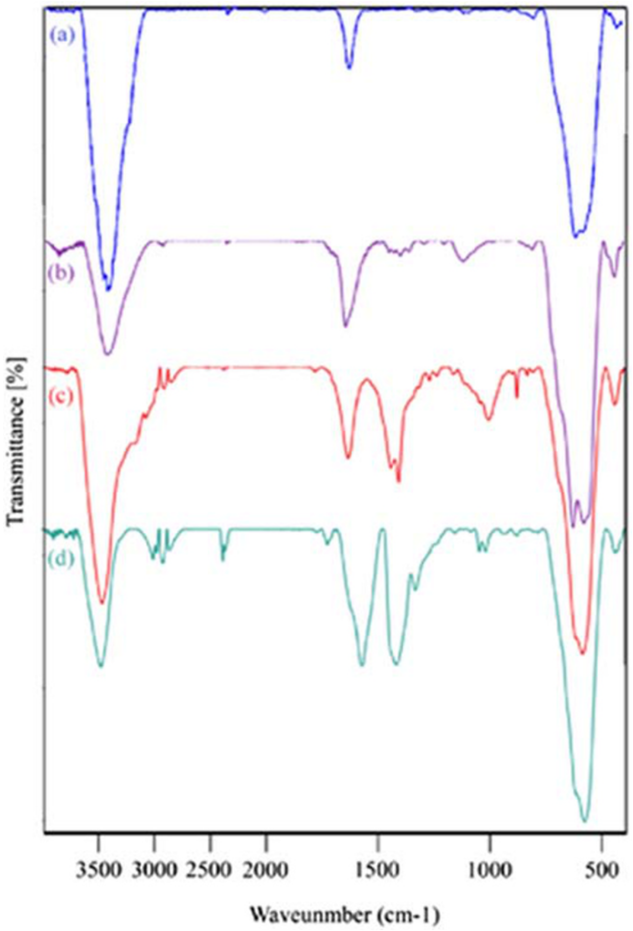

FIGURE 4 FT-IR spectra of (a) Fe_3O_4 nanoparticles, (b) 3-CPTS/Fe_3O_4, (c) FB/MNP and (d) Pd-FB/MNP

The vibrating sample magnetometer (VSM) of Fe_3O_4 nanoparticles and Pd-FB/MNP were conducted at room temperature. According to the VSM diagrams (Figure 6), these compounds have neither remanence nor coercivity and exhibit superparamagnetic characteristics at room temperature. Pd-FB/MNP (60.05 emu g^{-1}) exhibit lower magnetic value compared to Fe_3O_4 nanoparticles (99.7 emu g^{-1}), which may be explained as a consequence of functionalization of Fe_3O_4 nanoparticles with non-magnetic materials like palladium complex.

In general, the specific BET surface area of the catalyst plays a crucial role in the enhancement of heterogeneously catalyzed organic reactions. In this regard, nitrogen

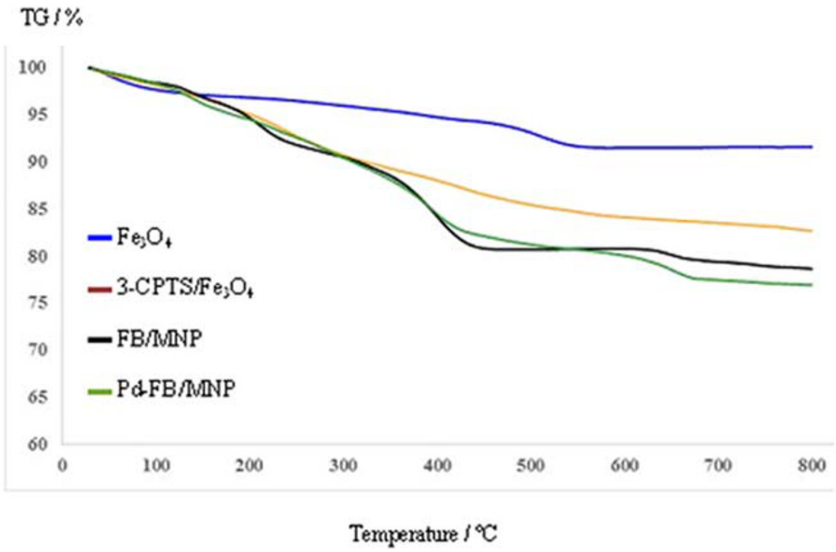

FIGURE 5 TGA curves of Fe_3O_4 nanoparticles, 3-CPTS/Fe_3O_4, FB/MNP and Pd-FB/MNP

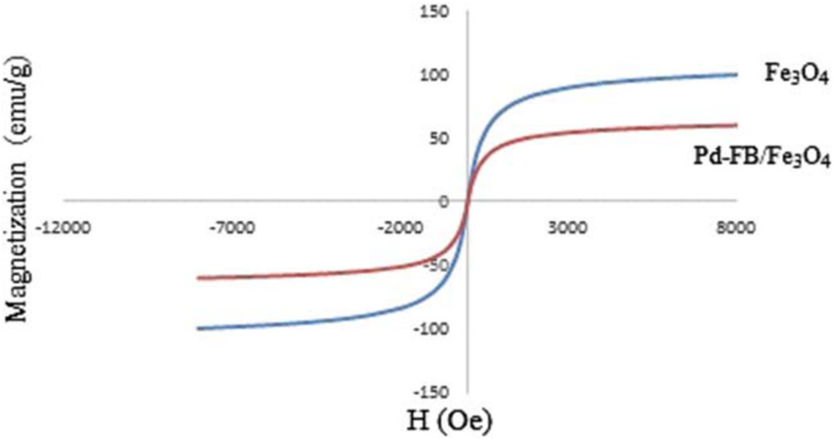

FIGURE 6 Magnetization hysteresis loops of Fe_3O_4 nanoparticles and Pd-FB/MNP

adsorption/desorption isotherms were used to determine the surface area of Pd-FB/MNP. N_2 adsorption/desorption measurements demonstrate the type IV isotherm with H_3 hysteresis loop illustrating the presence of mesopores (Figure 7). The specific surface area of Pd-FB/MNP was calculated to be 38.45 m^2/g using Brunauer–Emmett–Teller (BET) method. On the other hand, the surface area of Fe_3O_4 nanoparticles is reported to be 57.54 m^2/g.[51] Apparently, the surface area of Pd-FB/MNP was significantly decreased via Fe_3O_4 functionalization indicating the stabilization of organic layers including palladium complex on the surface of Fe_3O_4 nanoparticles.

3.2 | Catalytic activity of Pd-FB/MNP in Suzuki and Stille reactions

The catalytic activity of Pd-FB/MNP has been investigated in Suzuki and Stille carbon–carbon coupling reactions.

To evaluate the efficiency of Pd-FB/MNP, the coupling of iodobenzene (1 mmol) and phenylboronic acid (1 mmol) was studied as a model reaction. In order to

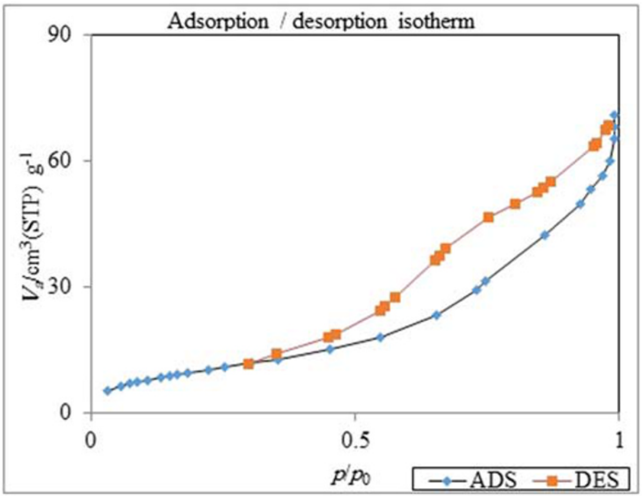

FIGURE 7 N_2 adsorption–desorption isotherm of Pd-FB/MNP

determine the optimum reaction conditions, the reaction temperature, the amount of catalyst and the effect of solvent and base were investigated and the results based on product yield are summarized in Table 1.

In an initial study, the reaction temperature was optimized within a temperature range of 25 to 80 °C in the presence of 15 mg of catalyst, Na_2CO_3 as base and PEG-400 as solvent (Table 1, entries 1–3). While the poor yield of product was observed up to 60 °C, the reaction yield sharply increased at 80 °C leading to excellent yield (98%).

The model reaction was studied in the absence and presence of the catalyst (Table 1, entries 4 and 5). No product was obtained in the absence of the catalyst even after long reaction time (24 hr), whereas the use of 10 mg of catalyst led to the formation of product after 70 min in high yield (90%). The effect of the amount of catalyst was determined from three reactions containing 10, 15 and 20 mg of Pd-FB/MNP (Table 1, entries 5–7). In the presence of 15 and 20 mg of catalyst, faster completion of the reaction was observed (40 min). The optimum amount of Pd-FB/MNP was found to be 15 mg of catalyst containing 0.0276 mmol of Pd per one mmol of substrate (phenylboronic acid) (Table 1, entry 6) leading to a quantitative yield of biphenyl.

The same reaction was carried out in the presence of various solvents such as H_2O, DMF, DMSO and PEG-400 (Table 1, entries 8–11). The excellent yield of product (98%) was obtained using DMF, DMSO, and PEG-400 in 40 min. Due to the toxicity of DMF and DMSO in comparison to PEG-400 (known as a green solvent), the use of the formers is not recommended. Therefore, PEG-400 was chosen as the optimum solvent.

Finally, the synthesis of biphenyl was also performed in the presence of common bases such as NaOEt, NaOH, Et_3N, and Na_2CO_3 (Table 1, entries 12–15). Among these bases, Na_2CO_3 proved to be the most effective one on the basis of shorter reaction time (40 min) and excellent yield (98%).

TABLE 1 Optimization of Suzuki coupling reaction in the presence of Pd-FB/MNP[a]

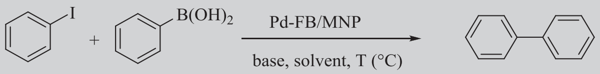

Entry	Catalyst (mg)	Solvent	Base	Temperature (°C)	Time (min)	Yield (%)[b]
Temperature effect						
1	15	PEG-400	Na_2CO_3	r.t.	60	Trace
2	15	PEG-400	Na_2CO_3	60	60	31
3	15	PEG-400	Na_2CO_3	80	40	98
Catalyst amount						
4	-	PEG-400	Na_2CO_3	80	24 h	-
5	10	PEG-400	Na_2CO_3	80	70	90
6	15	PEG-400	Na_2CO_3	80	40	98
7	20	PEG-400	Na_2CO_3	80	40	98
Solvent effect						
8	15	H_2O	Na_2CO_3	80	70	63
9	15	DMF	Na_2CO_3	80	40	98
10	15	DMSO	Na_2CO_3	80	40	98
11	15	PEG-400	Na_2CO_3	80	40	98
Base effect						
12	15	PEG-400	NaOEt	80	60	Trace
13	15	PEG-400	NaOH	80	60	53
14	15	PEG-400	Et_3N	80	60	49
15	15	PEG-400	Na_2CO_3	80	40	98

[a] Reaction conditions: iodobenzene (1 mmol), phenylboronic acid (1 mmol), base (3 mmol) and solvent (1 ml),
[b] Isolated yield.

TABLE 2 Suzuki C-C coupling reaction of aryl halides using phenylboronic acid in the presence of Pd-FB/MNP[a]

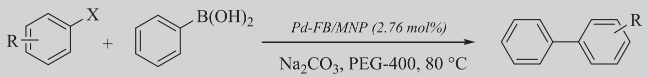

X= Br, I

Entry	Aryl halide	Product	Time (min)	Yield (%)[b]	TON	M.p. (°C)	M.p. (°C)[Ref.]
1	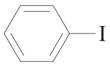	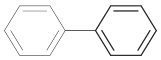	40	98	35.5	64–66	64–66[48]
2	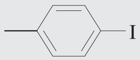	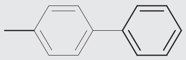	40	93	33.7	41–44	42–43[48]
3	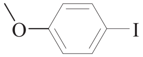	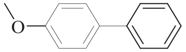	150	91	32.9	82–85	81–83[48]
4	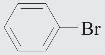	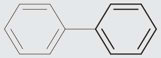	55	88	31.9	64–66	63–65[48]
5	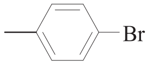	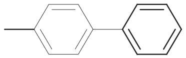	60	90	32.6	41–44	42–43[48]
6	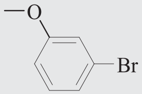	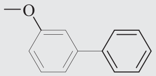	135	87	31.5	Oil	Oil[52]

TABLE 2 (Continued)

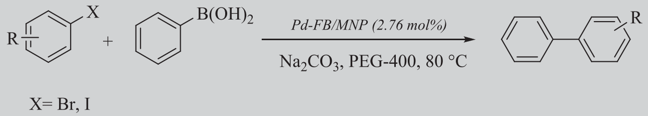

Entry	Aryl halide	Product	Time (min)	Yield (%)[b]	TON	M.p. (°C)	M.p. (°C)[Ref.]
7	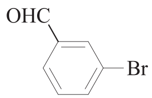	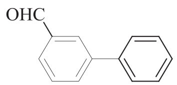	130	90	32.6	Oil	Oil[52]
8	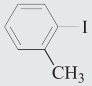	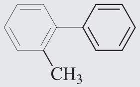	215	93	33.7	Oil	Oil[48]
9	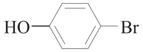	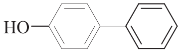	140	90	32.6	161–164	161–163[49]
10	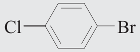	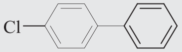	30	96	34.8	70–72	70–72[48]
11	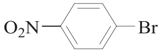	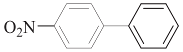	30	96	34.8	111–114	112–115[48]
12	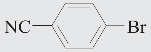	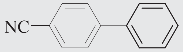	30	90	32.6	81–83	82–83[48]

(Continues)

TABLE 2 (Continued)

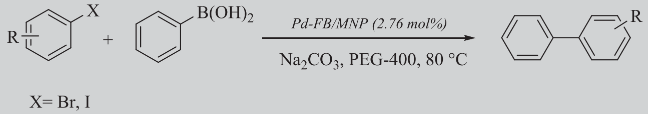

Entry	Aryl halide	Product	Time (min)	Yield (%)[b]	TON	M.p. (°C)	M.p. (°C)[Ref.]
13	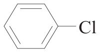	-	24 hr	-	-	-	-

[a] Reaction conditions: aryl halide (1 mmol), phenylboronic acid (1 mmol), Na_2CO_3 (3 mmol), Pd-FB/MNP (15 mg catalyst contains 0.0276 mmol Pd), reaction temperature 80 °C and PEG-400 (1 ml).

[b] Isolated yield. TON (turnover number = mmol of product/mmol of catalyst).

TABLE 3 Stille C-C coupling reaction of aryl halides using triphenyltin chloride in the presence of Pd-FB/MNP[a]

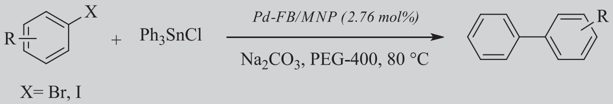

Entry	Aryl halide	Product	Time (min)	Yield (%)[b]	TON	M.p. (°C)	M.p. (°C)[Ref.]
1	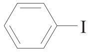	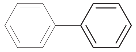	75	95	34.4	64–66	64–66[48]
2	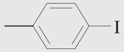	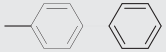	90	95	34.4	41–44	42–43[48]

TABLE 3 (Continued)

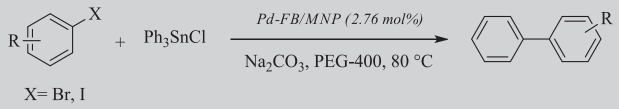

Entry	Aryl halide	Product	Time (min)	Yield (%)[b]	TON	M.p. (°C)	M.p. (°C)[Ref.]
3	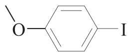	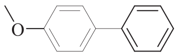	255	96	34.8	82–84	81–83[48]
4	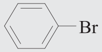	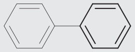	115	91	32.9	64–66	63–65[48]
5	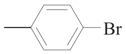	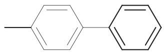	100	92	33.3	41–43	42–43[48]
6	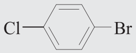	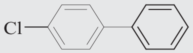	60	93	33.7	70–72	70–72[48]
7	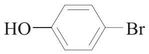	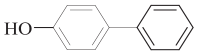	220	88	31.9	161–164	161–163[49]
8	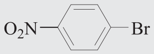	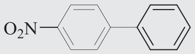	70	91	32.9	111–114	112–115[48]
9	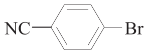	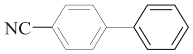	65	97	35.1	81–83	82–83[48]

(Continues)

TABLE 3 (Continued)

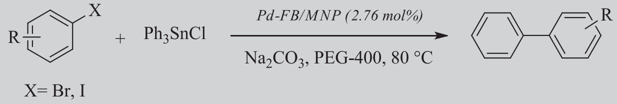

Entry	Aryl halide	Product	Time (min)	Yield (%)[b]	TON	M.p. (°C)	M.p. (°C)[Ref.]
10	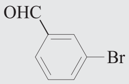	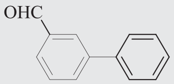	185	90	32.6	Oil	Oil[52]
11	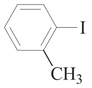	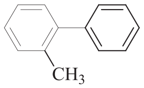	260	93	33.7	Oil	Oil[48]

[a] Reaction conditions: aryl halide (1 mmol), triphenyltin chloride (0.5 mmol), Na_2CO_3 (3 mmol), Pd-FB/MNP (15 mg catalyst contains 0.0276 mmol Pd), reaction temperature 80 °C and PEG-400 (1 mL).

[b] Isolated yield. TON (turnover number = mmol of product/mmol of catalyst).

Accordingly, the reaction containing Pd-FB/MNP (15 mg) as a catalyst at 80 °C after 40 min exhibited the highest isolated yield and afforded the product (biphenyl) quantitatively (Table 1, entry 3).

After obtaining the best reaction conditions, a variety of aryl halides bearing electron-donating (hydroxyl, methoxy, and methyl) and electron-withdrawing (chloro, cyano, carbonyl, and nitro) substituents were investigated to confirm the generality of the present method. As depicted in Table 2, all biphenyl products were obtained in high to excellent yields and TON values, although the reaction time depended strongly on the nature of substituents. The results revealed that this methodology is effective for phenyl iodide (Table 2, entry 1) and -bromide (Table 2, entry 4). On the contrary, phenyl chloride (Table 2, entry 13) showed no reactivity towards the coupling reaction. In this regard, we found that the chloro functional group remained intact during the C-C coupling reactions (Table 2, entry 10). This limitation might be an important advantage of the presented method since selectivity is an important factor in catalytic systems.

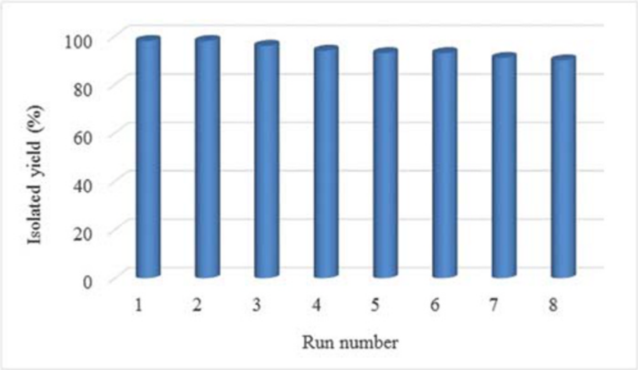

FIGURE 8 Recyclability of Pd-FB/MNP in the coupling reaction of iodobenzene with PhB $(OH)_2$

To extend the scope of activity of the catalyst, it was also tested for Stille C-C coupling of a variety of aryl halides with triphenyltin chloride (Ph_3SnCl) in a molar ratio of 1:0.5 under optimized reaction conditions. As depicted in Table 3, the biphenyl derivatives were obtained in high to excellent yields and TON values for aryl halides containing either electron-rich or electron-deficient substituents. The high value of TON confirms the excellent catalytic activity of Pd-FB/MNP in coupling reactions. While the same trend is observed for Stille and Suzuki coupling reaction, Stille reaction requires a longer reaction time. Interestingly, this reaction showed also the same selectivity towards chloro substituted aryl bromide (Table 3, entry 7).

Reusability of the catalysts is an important factor in the field of heterogeneous catalysis. To investigate this issue, the recyclability of Pd-FB/MNP catalyst has been studied in the coupling reaction of iodobenzene with phenylboronic acid as a model reaction. After completion of the reaction, the catalyst was removed readily from the reaction mixture using an external magnetic bar, washed with diethyl ether, and reused for a subsequent run. As depicted in Figure 8, Pd-FB/MNP can be reused up to eight times without significant loss in catalytic activity (product yield: 98% for the first run; 90% for the eighth run).

To confirm the sustainable nature of Pd-FB/MNP, the leaching test was performed for the optimized Suzuki coupling model reaction (Table 2, entry 1). For this purpose, two parallel reactions were carried out. In the first reaction, 60% of biphenyl product was obtained in half-time of reaction (20 min), whereas in the second reaction, catalyst was removed after 20 min and the reaction was

TABLE 4 A comparison study of Pd-FB/MNP in the Suzuki coupling reaction of iodobenzene with phenylboronic acid with previously reported catalysts

Entry	Catalyst	Reaction conditions	Time (min)	Yield (%) [Ref.]
1	PANI-Pd	K_2CO_3, 1,4-dioxane: H_2O (1:1), 95 °C	240	91[53]
2	N,N′-bis(2-pyridinecarboxamide)-1,2-benzene Pd complex	H_2O, K_2CO_3, 100 °C	180	97[54]
3	NHC-Pd (II) complex	THF, Cs_2CO_3, 80 °C	12 h	88[55]
4	Au/Pd NPs	EtOH/H_2O, K_2CO_3, 80 °C	24 h	88[56]
5	Pd NP	H_2O, KOH, 100 °C	12 h	95[57]
7	Polymer anchored Pd (II) Schiff base complex	K_2CO_3, DMF: H_2O (1:1), 80 °C	300	99[58]
8	Pd/SBA-15/IL DABCO	K_2CO_3, H_2O, 80 °C	90	97[59]
9	SBA-16-2 N-Pd (II)	EtOH, K_2CO_3, 60 °C	120	99[60]
10	Pd-FB/MNP	PEG-400, Na_2CO_3, 80 °C	40	98[this work]

then allowed to continue without catalyst. In this stage, 63% of biphenyl product (instead of 98%) was obtained. These experiments confirm that the leaching of palladium does not occur during the reaction.

The results obtained from Suzuki coupling reaction of iodobenzene with PhB $(OH)_2$ using various Pd heterogeneous *catalysts* including Pd-FB/MNP are summarized in Table 4. This protocol has attractive features in terms of reaction rate, product yield, and easy magnetic separation when compared with other ones.

4 | CONCLUSIONS

Pd-FB/MNP has been introduced as a novel magnetically retrievable nanoparticle material. Its formation has been confirmed by spectroscopic techniques such as FT-IR, SEM, TGA, XRD, ICP, EDS, BET and VSM. The viability of Pd-FB/MNP as a catalyst has been investigated for Suzuki and Stille C-C coupling reactions in a mild basic green media (Na_2CO_3 in PEG-400). Also, selective formation of biphenyl derivatives from aryl iodides and bromides was successfully achieved. The attractive features of this phosphine- and halide-free protocol remain in its relatively low palladium loading (2.76 mol%), facile recovery of the catalyst (using an external magnet) and its non-leaching nature and its high performance even after eight consecutive reaction cycles (90%). The coordination of Pd to fuberidazole as a novel immobilized chelating agent (bearing N in the benzimidazolium core and O in its furyl one) may open new venues for the design of analogous materials and various purposes.

ORCID

Mitra Ghassemzadeh https://orcid.org/0000-0002-6394-571X

Maryam Afsharpour https://orcid.org/0000-0002-5672-7546

REFERENCES

[1] S. Zhao, B. Xu, L. Yu, Y. Fan, *Chin. Chem. Lett.* **2018**, *29*, 475.
[2] D. Zhang, Z. Wei, L. Yu, *Sci. Bull.* **2017**, *62*, 1325.
[3] S. Zhao, B. Xu, L. Yu, Y. Fan, *Chin. Chem. Lett.* **2018**, *29*, 884.
[4] G. Sartori, R. Ballini, F. Bigi, G. Bosica, R. Maggi, P. Righi, *Chem. Rev.* **2004**, *104*, 199.
[5] Á. Molnár, B. Rác, *Curr. Org. Chem.* **2006**, *10*, 1697.
[6] S. Dasgupta, B. Török, *Org. Prep. Proc. Int.* **2008**, *40*, 1.
[7] M. J. Climent, A. Corma, S. Iborra, *Chem. Rev.* **2011**, *111*, 1072.
[8] A. H. M. Elwahy, M. R. Shaaban, *RSC Adv.* **2015**, *5*, 75659.
[9] Y. Yang, B. Xu, J. He, J. Shi, L. Yu, Y. Fan, *Appl. Organomet. Chem.* **2019**, *33*, e5204.
[10] E. L. Downs, D. R. Tyler, *Coord. Chem. Rev.* **2014**, *280*, 28.
[11] V. Polshettiwar, R. Luque, A. Fihri, H. Zhu, M. Bouhrara, J. M. Basset, *Chem. Rev.* **2011**, *111*, 3036.
[12] L. M. Rossi, N. J. S. Costa, F. P. Silva, R. Wojcieszak, *Green Chem.* **2014**, *16*, 2906.
[13] J. Govan, Y. K. Gun'ko, *Nanomaterials* **2014**, *4*, 222.
[14] R. K. Sharma, S. Dutta, S. Sharma, R. Zboril, R. S. Varma, M. B. Gawande, *Green Chem.* **2016**, *18*, 3184.
[15] T. Cheng, D. Zhang, H. Li, G. Liu, *Green Chem.* **2014**, *16*, 3401.
[16] P. Das, W. Linert, *Coord. Chem. Rev.* **2016**, *311*, 1.
[17] L. Dalla-Vechia, B. Reichart, T. Glasnov, L. S. M. Miranda, C. O. Kappe, R. O. M. A. de Souza, *Org. Biomol. Chem.* **2013**, *11*, 6806.
[18] T. Leermann, P.-E. Broutin, F. R. Leroux, F. Colobert, *Org. Biomol. Chem.* **2012**, *10*, 4095.
[19] M. C. Bagley, M. Baashen, I. Chuckowree, J. E. Dwyer, D. Kipling, T. Davis, *Pharmaceuticals* **2015**, *8*, 257.
[20] S. Sobhani, Z. Zeraatkar, F. Zarifi, *New J. Chem.* **2015**, *39*, 7076.
[21] P. Mondal, R. Khatun, P. Bhanja, A. Bhaumik, D. Das, S. Manirul Islam, *J. Colloid Interface Sci.* **2017**, *508*, 378.
[22] J. Mondal, A. Modak, A. Bhaumik, *J. Mol. Catal. A: Chem.* **2011**, *350*, 40.
[23] M. O. Sydnes, *Catalysts* **2017**, *7*, 35.
[24] K. Aghapoor, F. Mohsenzadeh, H. Sayahi, S. Rastgar, H. R. Darabi, *Environ. Chem. Lett.* **2018**, *16*, 1109.
[25] F. Téllez, H. López-Sandoval, S. E. Castillo-Blum, N. Barba-Behrens, *Arkivoc* **2007**, *2008*, 245. https://doi.org/10.3998/ark.5550190.0009.519
[26] H. Liu, B. Zhang, C. Tan, F. Liu, J. Cao, Y. Tan, Y. Jiang, *Talanta* **2016**, *161*, 309.
[27] E. Horak, P. Kassal, I. Murković Steinberg, *Supramol. Chem.* **2018**, *30*, 838.
[28] F. A. S. Chipem, S. Kumar Behera, G. Krishnamoorthy, *Sens. Actuators B* **2014**, *191*, 727.
[29] K. Akutsu, S. Mori, K. Shinmei, H. Iwase, Y. Nakano, Y. Fujii, *Talanta* **2016**, *146*, 575.
[30] N. Manojai, R. Daengngern, K. Kerdpol, C. Ngaojampa, N. Kungwan, *J. Luminescence* **2017**, *188*, 275.
[31] M. Qin, D. Jin, W. Che, Y. Jiang, L. Zhang, D. Zhu, Z. Su, *Inorg. Chem. Commun.* **2017**, *75*, 25.
[32] D. Y. Lee, N. Singh, D. O. Jang, *Tetrahedron Lett.* **2010**, *51*, 1103.
[33] P. Saluja, N. Kaur, N. Singh, D. O. Jang, *Tetrahedron Lett.* **2012**, *53*, 3292.
[34] P. Saluja, N. Kaur, N. Singh, D. O. Jang, *Tetrahedron* **2012**, *68*, 8551.
[35] L. Tang, M. Cai, Z. Huang, K. Zhong, S. Hou, Y. Bian, R. Nandhakumar, *Sens. Actuators B* **2013**, *185*, 188.
[36] A. Tavman, I. Boz, A. S. Birteksöz, A. Cinarli, *J. Coord. Chem.* **2010**, *63*, 1398.
[37] A. Tavman, A. Çinarli, D. Gürbüz, A. S. Birteksöz, *J. Iran. Chem. Soc.* **2012**, *9*, 815.
[38] D. A. M. Watkins, *Pestic. Sci.* **1976**, *7*, 184.
[39] K. Bramhanwade, S. Shende, S. Bonde, A. Gade, M. Rai, *Environ. Chem. Lett.* **2016**, *14*, 229.
[40] M. Rai, A. P. Ingle, P. Paralikar, N. Anasane, R. Gade, P. Ingle, *Appl. Microbiol. Biotechnol.* **2018**, *102*, 6827.
[41] R. B. Nasir Baig, R. S. Varma, *Chem. Commun.* **2013**, *49*, 752.

[42] M. B. Gawande, P. S. Branco, R. S. Varma, *Chem. Soc. Rev.* **2013**, *42*, 3371.

[43] A. H. M. Elwahy, M. R. Shaaban, *Heterocycles* **2017**, *94*, 595.

[44] M. Ghassemzadeh, S. Bahemmat, M. Mahmoodabadi, B. Rezaii-Rad, H. H. Monfared, E. Mottefakeri, B. Neumüller, *Polyhedron* **2010**, *29*, 3036.

[45] M. Ghassemzadeh, S. Bahemmat, M. Tabatabaee, S. Nassiri, B. Neumüller, *Polyhedron* **2011**, *30*, 1760.

[46] A. Gouranourimi, M. Ghassemzadeh, S. Bahemmat, B. Neumüller, R. Tonner, *Monatsh. Chem.* **2015**, *146*, 57.

[47] S. Bahemmat, M. Ghassemzadeh, M. Afsharpour, K. Harms, *Synthesis, Polyhedron* **2015**, *89*, 196.

[48] A. Ghorbani-Choghamarani, B. Tahmasbi, N. Noori, R. Ghafouri-nejad, *J. Iran. Chem. Soc.* **2017**, *14*, 681.

[49] A. Ghorbani-Choghamarani, B. Tahmasbi, N. Noori, S. Faryadi, *C. R. Chim.* **2017**, *20*, 132.

[50] M. Kidwai, A. Jahan, D. Bhatnagar, *J. Chem. Sci.* **2010**, *122*, 607.

[51] Y. Liu, P. Liu, Z. Su, F. Li, F. Wen, *Appl. Surf. Sci.* **2008**, *255*, 2020.

[52] A. Ghorbani-Choghamarani, B. Tahmasbi, Z. Moradi, *Appl. Organomet. Chem.* **2017**, *31*, e3665.

[53] H. A. Patel, A. L. Patel, A. V. Bedekar, *Appl. Organomet. Chem.* **2015**, *29*, 1.

[54] M. Gholinejad, H. R. Shahsavari, *Inorg. Chim. Acta* **2014**, *421*, 433.

[55] T. Chen, J. Gao, M. Shi, *Tetrahedron* **2006**, *62*, 6289.

[56] M. Nasrollahzadeh, A. Azarian, M. Maham, A. Ehsani, *J. Ind. Eng. Chem.* **2015**, *21*, 746.

[57] M. Nasrollahzadeh, S. M. Sajadi, M. Maham, *J. Mol. Catal. A: Chem.* **2015**, *396*, 297.

[58] S. M. Islam, A. S. Roy, P. Mondal, N. Salam, *Appl. Organomet. Chem.* **2012**, *26*, 625.

[59] S. Rostamnia, E. Doustkhah, B. Zeynizadeh, *Microporous Mesoporous Mater.* **2016**, *222*, 87.

[60] H. B. Wang, Y. H. Zhang, H. L. Yang, Z. Y. Ma, F. W. Zhang, J. Sun, J. T. Ma, *Mesoporous Microporous Mater.* **2013**, *168*, 65.

How to cite this article: Nouri K, Ghassemzadeh M, Mohsenzadeh F, Afsharpour M. Pd(0) complex of fuberidazole modified magnetic nanoparticles: A novel magnetically retrievable high-performance catalyst for Suzuki and Stille C-C coupling reactions. *Appl Organomet Chem*. 2020;e5771. https://doi.org/10.1002/aoc.5771